Journal of Power Sources 234 (2013) 175–179

Contents lists available at SciVerse ScienceDirect

Journal of Power Sources

journal homepage: www.elsevier.com/locate/jpowsour

Short communication

$Na_4Co_3(PO_4)_2P_2O_7$: A novel storage material for sodium-ion batteries

Masafumi Nose*, Hideki Nakayama, Kunihiro Nobuhara, Hiroyuki Yamaguchi, Shinji Nakanishi, Hideki Iba

Toyota Motor Corporation, Battery Research Division, 1200 Mishuku, Susono, Shizuoka 410-1193, Japan

HIGHLIGHTS

- A novel storage material $Na_4Co_3(PO_4)_2P_2O_7$ was prepared by a typical sol–gel method.
- Multistep redox behavior was confirmed in the high potential region between 4.1 V and 4.7 V *vs.* Na^+/Na.
- The reversible capacity of $Na_4Co_3(PO_4)_2P_2O_7$ reaches ca. 95 $mAhg^{-1}$.
- $Na_4Co_3(PO_4)_2P_2O_7$ exhibits the compatibility of high operating potential and high rate capabilities.

GRAPHICAL ABSTRACT

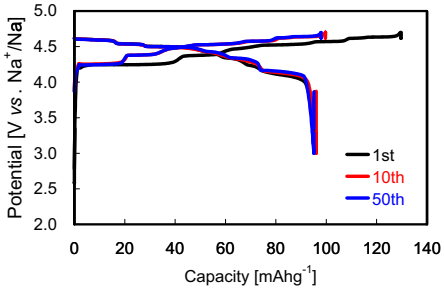

ARTICLE INFO

Article history:
Received 16 January 2013
Accepted 28 January 2013
Available online 9 February 2013

Keywords:
Sodium-ion battery
High potential
Multistep redox reaction
High rate capability
$Na_4Co_3(PO_4)_2P_2O_7$

ABSTRACT

The electrochemical properties of $Na_4Co_3(PO_4)_2P_2O_7$ as a positive electrode for sodium-ion batteries were characterized by a cyclic voltammetry technique and galvanostatic charge/discharge tests. Interestingly, $Na_4Co_3(PO_4)_2P_2O_7$ has the multi redox couples in the highest potential region between 4.1 V and 4.7 V among ever reported sodium storage materials and can deliver the reversible capacity of ca. 95 $mAhg^{-1}$, corresponding to ca. 2.2 Na^+ extraction and insertion in $Na_4Co_3(PO_4)_2P_2O_7$, at the current density of 34 mAg^{-1} (0.2 C). $Na_4Co_3(PO_4)_2P_2O_7$ also exhibits the high rate capabilities and has a small polarization in the charge–discharge profile even at the high current densities of 4.25 Ag^{-1} (25 C), resulting in high energy efficiency of the battery. These performances indicate $Na_4Co_3(PO_4)_2P_2O_7$ can be one of the good candidates for a positive electrode material of sodium-ion batteries.

© 2013 Elsevier B.V. All rights reserved.

1. Introduction

Lithium-ion batteries (LIBs) have been well established as power sources of portable electric devices for the last 20 years because of their high energy density, light weight, long cycle life and so on. To date, LIBs have diversified their applications not only as large-scale power sources of hybrid vehicles (HVs), plug-in hybrid vehicles (PHVs) and electric vehicles (EVs) but also as back up storage systems of solar and wind energies. In order to meet the requirements, much effort has been devoted on the new types of rechargeable batteries (e.g. other alkali-ion batteries, all solid batteries and lithium-air batteries). The variety of batteries will permit the diverse applications and will make it possible to build up a sustainable society with green chemistry. Especially, high power of the battery ($W = V \times I$), which can be achieved by high operating voltage (V) and high rate capability (I), has been desired to further enhance the fuel and/or electrical efficiency of upcoming system, which are so-called "energy efficiency".

In rocking chair type lithium- and sodium-ion batteries, the rate capability is determined by any one of the following rate-limiting step; (1) ion transport at the interface between electrolyte and storage material and (2) ion diffusion in the bulk of storage material [1–3]. In typical LIBs, the rate-limiting step comes from the electrolyte/storage material interface, because an interaction between

* Corresponding author.
E-mail address: nose@masafumi.tec.toyota.co.jp (M. Nose).

0378-7753/$ – see front matter © 2013 Elsevier B.V. All rights reserved.
http://dx.doi.org/10.1016/j.jpowsour.2013.01.162

mobile ion and solvent has a kinetically strong influence on the interfacial ion transport. Actually, a few fundamental studies have indicated that the interfacial Na^+ transport should be kinetically rapid as compared with Li^+, because Lewis acidity of Na^+ is inherently weaker than that of Li^+ and therefore the interaction of Na^+ and solvent becomes weaker [2,3]. This evidence suggests that sodium-ion batteries using Na^+ as a career instead of Li^+ must have a potential of fast ion transport even at the interface. Owing to such a positive advantage, lots of sodium storage materials have been intensively studied and optimized their better performances. Nowadays, various sodium storage materials have been reported not only for a positive electrode (e.g. layered oxides [4–6] and phosphates [7–11]) but also a negative electrode (e.g. carbonaceous materials [12,13] and titanium oxides [14–16]). This wide selectivity is characteristic of sodium-ion batteries. However, sodium storage materials for a positive electrode with both high potential and high Na^+ diffusivity in the bulk, which are also parameters to determine high power of the battery, have not been found yet. Researches on the compatible storage material for a positive electrode are one of the most important issues to establish higher power type sodium-ion batteries.

Maricite $NaCoPO_4$ may have a high operating potential beyond 4.0 V *vs.* Na^+/Na from material screening done by DFT calculation [17]. High redox potential of Co^{2+}/Co^{3+} has been certainly induced by polyanion unit such as PO_4. However, from its structural viewpoint, maricite $NaCoPO_4$ may be electrochemically inactive because Na^+ are located in the enclosed framework and octahedral CoO_6 and polyhedral PO_4 units block the Na^+ diffusion. In LIBs, olivine $LiFePO_4$ is well known to electrochemically active because it has a one-dimensional (1D) Li^+ mobile route in the bulk [18]. These results suggest that the crystal structure will play an important role in mobile ion's diffusivity in the bulk. Herein, we have conducted material survey from various polymorphs of sodium-based cobalt phosphates, which might not be familiar with lithium-based ones. Among them, we focused on the unique crystal structure of $Na_4Co_3(PO_4)_2P_2O_7$ as described in Fig. 1. Here, the schematic illustrations of the crystal structure of $Na_4Co_3(PO_4)_2P_2O_7$ were drawn by using the program VESTA [19]. According to the several reports, $Na_4M_3(PO_4)_2P_2O_7$ [M = Co, Ni, Mn, Mg and Fe] has a space group of $Pn2_1a$ and $M_3P_2O_{13}$ blocks parallel to bc plane are linked with P_2O_7 unit along a-axis [11,20–22]. Interestingly, four types of Na^+ sites are located in the 3D ion channel. As compared with ion diffusivity in 1D ion channel, 3D ion channel would have great advantage on ion diffusivity because alternative diffusion pathways exist even if defects in bulk block ion mobility in one direction of 3D ion channel

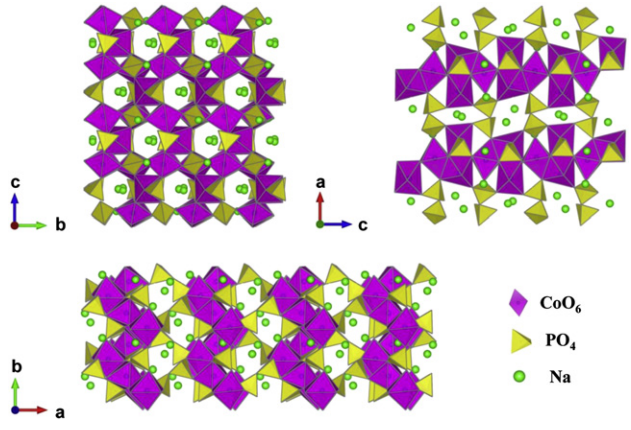

Fig. 1. Polyhedral view of $Na_4Co_3(PO_4)_2P_2O_7$ with $Pn2_1a$ space group along three different directions.

[18]. Therefore, the crystal structure of $Na_4Co_3(PO_4)_2P_2O_7$ can be very attractive to use as a positive electrode for sodium-ion batteries, and so we have investigated on the sodium intercalation capabilities of $Na_4Co_3(PO_4)_2P_2O_7$. In this paper, we describe the electrochemical properties of $Na_4Co_3(PO_4)_2P_2O_7$ as a positive electrode for sodium-ion batteries.

2. Experimental

$Na_4Co_3(PO_4)_2P_2O_7$ was synthesized by using a sol–gel method. Reagent grade of $(CH_3COO)_2Co$, $Na_4P_2O_7$ and $NH_4H_2PO_4$ (Nacali tesque) were used as the starting materials. These materials were mixed in a diluted nitric acid solution and then glycolic acid was added to prevent the particle growth of $Na_4Co_3(PO_4)_2P_2O_7$ precursor. The solution was heated at 80 °C for 12 h with continuous stirring. The gel obtained was annealed to 700 °C for 50hr under air atmosphere. After that, the active material and Vapor-Grown Carbon Fiber (Showa Denko, VGCF, battery grade) were mixed with a weight ratio of 5:1, and subsequently heat retreatment was carried out at 700 °C for 5 h under purging Ar. Then, a N-methyl pyrrolidone (NMP) based slurry composed of the mixture (90 wt%) of $Na_4Co_3(PO_4)_2P_2O_7$ and VGCF, acetylene black (battery grade, 5 wt %) as a conductive filler and poly(vinylidene fluoride) (battery grade, PVDF, 5 wt%) as a binder was cast on an aluminum current collector. The as-prepared material was characterized by powder X-ray diffraction measurements with X-ray diffractometer (Ultima IV, Rigaku corp. Ltd., Japan) using Cu Kα radiation with 40 kV of tube voltage and 40 mA of current. Surface morphology of the as-prepared material was obtained with a field emission scanning electron microscope (Ultra55, ZEISS).

CR2032-type coin cell was fabricated with the above-described positive electrode. Metallic sodium (Aldrich) was used as a negative electrode and 1.0 mol cm^{-3} $NaPF_6$ (Kishida Chem., battery grade) dissolved in ethylene carbonate (EC)/diethylene carbonate (DEC) (50:50 by vol., Kishida Chem., battery grade) was applied to the electrolyte. All electrochemical tests were conducted in a thermostatic bath maintaining at 25 °C. Cyclic voltammetry was measured at a constant scan rate of 0.01 mV s^{-1} in the potential region between 3.9 V and 4.8 V *vs.* Na^+/Na. Galvanostatic charge–discharge test was carried out at a constant current density of 34 mAg^{-1} (0.2 C) between 3.0 V and 4.7 V *vs.* Na^+/Na. 1 C was defined as the current density of 170 mAg^{-1}, at which its theoretical capacity (170 $mAhg^{-1}$) can be delivered for an hour. Rate performances were also evaluated between 2.0 V and 5.0 V *vs.* Na^+/Na at different current densities of 1.7 Ag^{-1} (10 C), 3.4 Ag^{-1} (20 C) and 4.25 Ag^{-1} (25 C). Practical sodium-ion battery was also assembled by combining $Na_4Co_3(PO_4)_2P_2O_7$ as a positive electrode and hard carbon (Kureha, battery grade) as a negative electrode. The negative electrode was composed of hard carbon (92.5 wt%) and PVdF binder (7.5 wt%) on a copper current collector. The battery performance was checked at a constant current density of 34 mAg^{-1} (0.2 C) in the voltage range between 3.0 V and 4.7 V.

3. Results and discussion

$Na_4Co_3(PO_4)_2P_2O_7$ was synthesized by a typical sol–gel method and subsequent heat treatment as described in the Experimental section. X-ray diffraction pattern and scanning electron microscope image shown in Figs. 2 and 3 indicated that as-prepared material had a main phase of $Na_4Co_3(PO_4)_2P_2O_7$ and a polycrystal with approximately 3 μm in diameter which was composed of submicron-sized primary particles. Fig. 4 shows the cyclic voltammograms (CVs) of $Na_4Co_3(PO_4)_2P_2O_7$ at the 2nd and 5th cycles between 3.9 V and 4.8 V *vs.* Na^+/Na at a sweeping rate of 0.01 mV s^{-1}. First redox couple corresponding to Na^+ extraction and

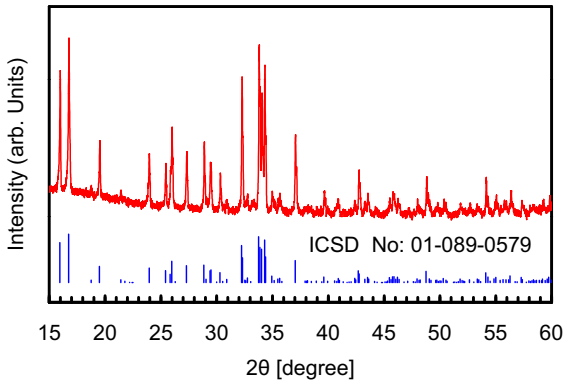

Fig. 2. Powder X-ray diffraction pattern of $Na_4Co_3(PO_4)_2P_2O_7$ between 15° and 60° (red line) with Bragg positions (blue line). (For interpretation of the references to color in this figure legend, the reader is referred to the web version of this article.)

insertion was confirmed at 4.26 V and 4.18 V *vs.* Na^+/Na, respectively. Then, multi redox couples appeared with an increase in the sweeping potential, and the highest redox potential was ca. 4.65 V and 4.62 V *vs.* Na^+/Na, respectively. No more reversible redox couple was obtained over 4.7 V *vs.* Na^+/Na, and then an irreversible oxidation current caused by the electrolyte decomposition gradually increased with an increase of the scanning potential up to 4.8 V *vs.* Na^+/Na. The CV curves at the 5th cycle was consistent with the 2nd one, which implies that the Na^+ extraction and insertion in the crystal structure of $Na_4Co_3(PO_4)_2P_2O_7$ can reversibly proceed. In addition, it should be emphasized that the overpotential of the first redox couple was roughly ±40 mV, while those of other redox couples were quite small (i.e. ±10–20 mV). This result suggests that sodium-ion diffusivity will strongly depends on Na^+ content and distribution in the bulk, and in particular, a fast Na^+ intercalation can be achieved in a specific structure where Na^+ is partially extracted. Olivine $LiFePO_4$ has only a kind of Li^+ site and a single Li^+ diffusion pathway, and shows a single redox couple around 3.45 V *vs.* Li^+/Li. The overpotential of $LiFePO_4$ was reported to be roughly ±65 mV [23] at the same scan rate (0.01 mV s^{-1}), which is much larger than that of $Na_4Co_3(PO_4)_2P_2O_7$. Herein, it is highly possible that small overpotential of $Na_4Co_3(PO_4)_2P_2O_7$ is delivered by arbitrarily distributed redox potentials in the charge–discharge process, and is also derived from a variety of Na^+ sites and multiple diffusion pathways in the structure.

Next, we conducted galvanostatic charge and discharge tests of $Na_4Co_3(PO_4)_2P_2O_7$. The potential limits were set at 3.0 V and 4.7 V *vs.* Na^+/Na and the current density was at a constant current density of 34 mAg^{-1} (0.2 C). As shown in Fig. 5a, reversible capacity of $Na_4Co_3(PO_4)_2P_2O_7$ reaches ca. 95 $mAhg^{-1}$, corresponding more than half of its theoretical capacity of 170 mAg^{-1}. Note that

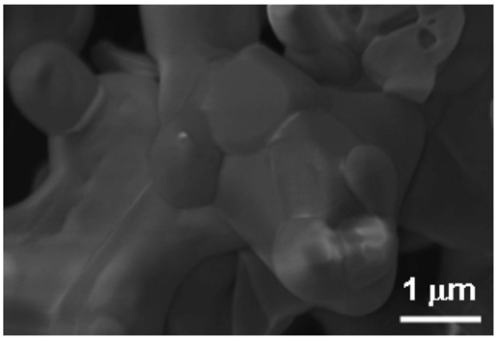

Fig. 3. Surface morphology of $Na_4Co_3(PO_4)_2P_2O_7$ obtained by a field-emission scanning electron microscope.

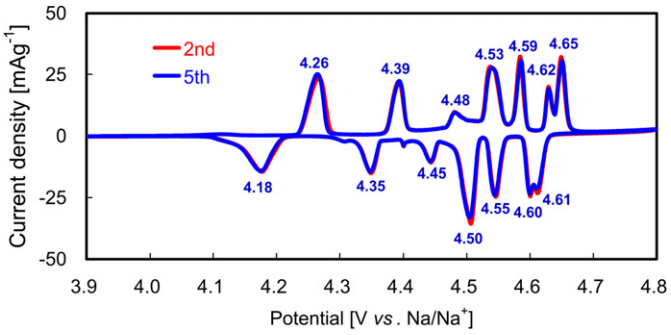

Fig. 4. Cyclic voltammograms of $Na_4Co_3(PO_4)_2P_2O_7$ at the 2nd and 5th cycles. The sweeping potential was between 3.9 V and 4.8 V *vs.* Na^+/Na at the rate of 0.01 mV s^{-1}.

$Na_4Co_3(PO_4)_2P_2O_7$ provides the 4.5 V-class highest average potential among ever reported Na^+ intercalation materials and the capacity fading is negligible even after 100th cycles. Fig. 6 shows the rate capabilities of $Na_4Co_3(PO_4)_2P_2O_7$ at different rates of 1.7 Ag^{-1} (10 C), 3.4 Ag^{-1} (20 C) and 4.25 Ag^{-1} (25 C) under the potential limits of 2.0 V and 5.0 V *vs.* Na^+/Na. Surprisingly, the reversible capacity reached ca. 80 $mAhg^{-1}$ even at 4250 mAg^{-1}. This result verifies that large reversible capacity of ca. 80 $mAhg^{-1}$ can be delivered within 70 s. More interestingly, the polarization of the charge and discharge reactions, which is related with energy efficiency of the battery, is little enough to maintain the high average potential beyond 4.0 V *vs.* Na^+/Na even at 4.25 Ag^{-1}. As far as we know, no sodium storage material has been reported on the compatibility of high potential and high rate capability. As discussed in the results of the CVs, four types of Na^+ sites and multiple diffusion pathways in the bulk produce the distributed equilibrium redox potentials and fast redox reaction for each potential will occur

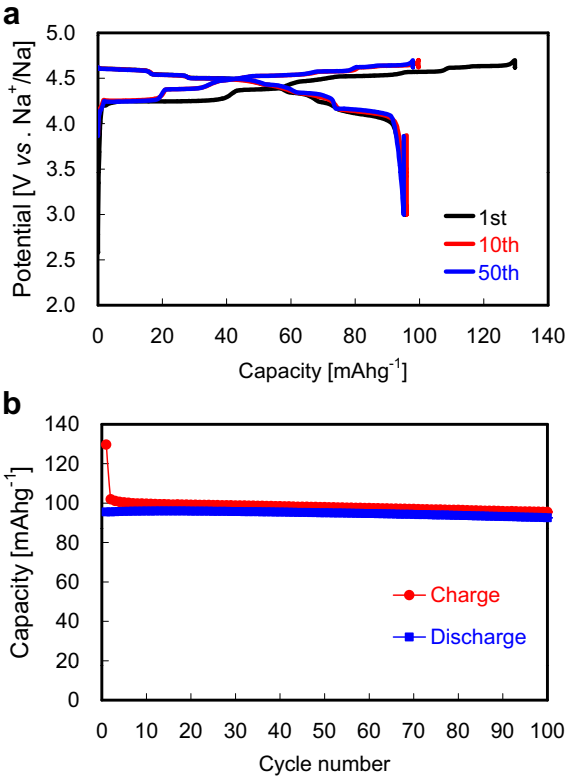

Fig. 5. a) Galvanostatic charge–discharge curves at 1st, 10th and 50th cycles and b) charge–discharge capacities as a function of cycle number of $Na_4Co_3(PO_4)_2P_2O_7$.

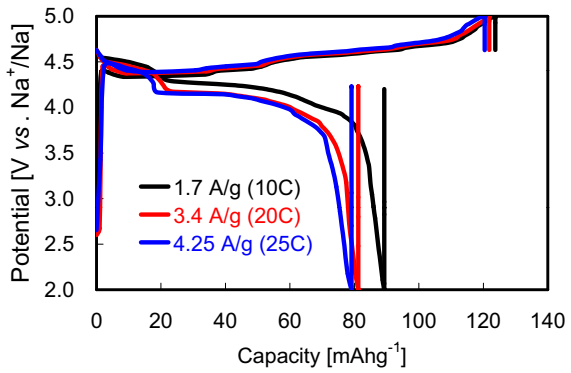

Fig. 6. Rate capabilities of $Na_4Co_3(PO_4)_2P_2O_7$ at the initial cycle under different current densities of 1.7 Ag^{-1} (10 C), 3.4 Ag^{-1} (20 C) and 4.25 Ag^{-1} (25 C).

because of the small overpotentials. Whereas the distributed redox reactions proceed separately at low rates as shown in the CVs, the new type of redox reaction occurs in parallel at high rates and then makes it possible to enhance notably the overall Na^+ diffusivity in the bulk. The diffusion behavior at high rates suggests that $Na_4Co_3(PO_4)_2P_2O_7$ has great advantages of rapid charge–discharge capability as well as high energy efficiency.

For the future, we will face on a remaining issue, which is to increase the reversible capacity in this intercalation structure, ultimately close to its theoretical capacity of 170 $mAhg^{-1}$. To achieve the theoretical value, ca. 33% of the initial Co must be oxidized from Co^{2+} through Co^{3+} up to Co^{4+} for the charge compensation of 4 Na^+ extraction from $Na_4Co_3(PO_4)_2P_2O_7$. Now, the reversible capacity of

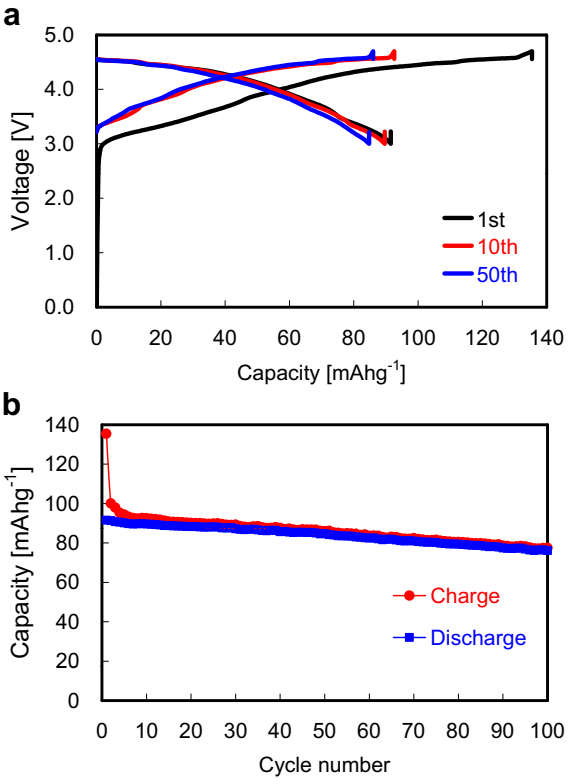

Fig. 7. a) Galvanostatic charge–discharge curves at 1st, 10th and 50th cycles and b) charge–discharge capacities as a function of cycle number of the practical sodium-ion battery using hard carbon as a negative electrode and $Na_4Co_3(PO_4)_2P_2O_7$ as a positive electrode.

95 $mAhg^{-1}$ at 34 $mAhg^{-1}$ (0.2 C) corresponds to about 2.2 Na^+ extraction and all the redox reaction is obtained up to 4.8 V *vs.* Na^+/Na as shown in the results of the CVs, indicating that Co^{2+}/Co^{3+} redox couple will be utilized in the charge–discharge reaction. Herein, the redox couple of Co^{3+}/Co^{4+} might be observed in the high potential region beyond 4.8 V *vs.* Na^+/Na. This potential is corresponding to ca. 5.1 V *vs.* Li^+/Li at which most of the organic electrolytes in LiBs are well understood to be unstable. Therefore, a suitable electrolyte having a wide potential window must be developed to activate further redox reaction of $Na_4Co_3(PO_4)_2P_2O_7$.

Finally, we have tried to construct the new type of practical sodium-ion battery by combining $Na_4Co_3(PO_4)_2P_2O_7$ as a positive electrode and hard carbon instead of Na metal as a negative electrode. Here, hard carbon has the large capacity of ca. 250 $mAhg^{-1}$ in the low potential region between 0.05 V and 1.0 V *vs.* Na^+/Na and therefore has been well-understood as one of the good candidates for a negative electrode material of sodium-ion batteries [12,13]. As shown in Fig. 7, this battery retained 4.0 V-class high voltage and exhibited the capacity retention of 93% at 50 cycles and 83% even at 100 cycles. The long-term stability implies that the Na^+ intercalation reaction between $Na_4Co_3(PO_4)_2P_2O_7$ and hard carbon reversibly occurred, and then encourages us to develop the practical sodium-ion battery system, which will compete with the performances of the state-of-art LIBs[26].

4. Conclusions

In this paper, we described the electrochemical properties of $Na_4Co_3(PO_4)_2P_2O_7$ as a positive electrode for sodium-ion batteries and the results of several electrochemical tests leaded to the following conclusions. Firstly, the reversible capacity of $Na_4Co_3(PO_4)_2P_2O_7$ reached ca. 95 $mAhg^{-1}$ with the 4.5 V-class highest average potential among ever reported sodium storage materials. Secondary, the rate performance of $Na_4Co_3(PO_4)_2P_2O_7$ shows the reversible capacity of ca. 80 $mAhg^{-1}$ can be delivered in just 70 s and the polarization is little enough to maintain the high discharge potential above 4.0 V *vs.* Na^+/Na. Finally, We could assemble a new type of sodium-ion batteries by combining $Na_4Co_3(PO_4)_2P_2O_7$ as a positive electrode and hard carbon as a negative electrode, and the battery shows the 4.0 V-class high operating voltage with the long-term operation. We believe these performances create a new perspective of sodium-ion batteries for the applications such as eco-friendly vehicles and other electric devices which require high power densities.

References

[1] B. Kang, G. Ceder, Nat. Lett. 458 (2009) 190–193.
[2] F. Sagane, T. Abe, Y. Iriyama, Z. Ogumi, J. Power Sources 146 (2005) 749–752.
[3] F. Sagane, T. Abe, Z. Ogumi, J. Power Sources 195 (2010) 7466–7470.
[4] Y. Kuroda, E. Kobayashi, S. Okada, J. Yamaki, ECS Meet. Abstr. (2010) 389.
[5] M. Sathiya, K. Hemalatha, K. Ramesha, J.M. Tarascon, A.S. Parkash, Chem. Mater. 24 (2012) 1846–1853.
[6] N. Yabuuchi, M. Kajiyama, J. Iwatate, H. Nishikawa, S. Hitomi, R. Okuyama, R. Usui, Y. Yamada, S. Komaba, Nat. Mater. 11 (2012) 512–517.
[7] N. Recham, J.-N. Chotard, L. Dupont, K. Djellab, M. Armand, J.M. Tarascon, J. Electrochem. Soc. 156 (2009) A993–A999.
[8] Y. Kawabe, N. Yabuuchi, M. Kajiyama, N. Fukuhara, T. Inamasu, R. Okuyama, I. Nakai, S. Komaba, Electrochem. Commun. 13 (2011) 1225–1228.
[9] J. Barker, M.Y. Swoyer, Electrochem. Solid-State Lett. 6 (2003) A1–A4.
[10] P. Barpanda, T. Ye, S. Nishimura, S.C. Chung, Y. Yamada, M. Okubo, H. Zhou, A. Yamada, Electrochem. Commun. 24 (2012) 116–119.
[11] H. Kim, I. Park, D.H. Seo, S. Lee, S.-W. Kim, W.J. Kwon, Y.U. Park, C.S. Kim, S. Jeon, K. Kang, J. Am. Chem. Soc. 134 (2012) 10369–10372.
[12] D.A. Stevens, J.R. Dahn, J. Electrochem. Soc. 147 (2000) 1271–1273.
[13] K. Gotoh, T. Ishikawa, S. Shimadzu, N. Yabuuchi, S. Komaba, K. Takeda, A. Goto, K. Deguchi, S. Ohki, K. Hashi, T. Shimizu, H. Ishida, J. Power Sources 225 (2013) 137–140.
[14] P. Senguttuvan, G. Rousse, V. Seznec, J.M. Tarascon, M. Rosa Palacín, Chem. Mater. 23 (2011) 4109–4111.

[15] N.D. Trinha, O. Crosniera, S.B. Schougaardb, T. Brousse, ECS Trans. 35 (2011) 91–98.
[16] L. Zhao, H.L. Pan, Y.S. Hu, H.C. Li, L.Q. Chen, Chin. Phys. B 21 (2012) 028201/1–028201/4.
[17] S.P. Ong, V.L. Chevrier, G. Hautier, A. Jain, C. Moore, S. Kim, X. Ma, G. Ceder, R. Soc. Chem. 4 (2011) 3680–3688.
[18] D. Morgan, A. Van der Ven, G. Ceder, Electrochem. Solid-State Lett. 7 (2004) A30–A32.
[19] K. Momma, F. Izumi, J. Appl. Crystallogr. 41 (2008) 653–658.
[20] F. sanz, C. parada, U. Amador, M.A. Monge, C. Ruiz-Valero, J. Solid State Chem. 123 (1996) 129–139.
[21] F. Sanz, C. Parada, J.M. Rojo, C. Ruiz-Valero, Chem. Mater. 13 (2001) 1334–1340.
[22] R. Essehlia, B.E. Bali, S. Benmokhtar, H. Fuessc, I. Svobodac, S. Obbaded, J. Alloys Compd. 493 (2010) 654–660.
[23] H.-C. Shin, W.-I. Cho, H. Jang, J. Power Sources 159 (2) (2006) 1383–1388.